Modern Chemistry
2015; 3(1-1): 15-26
Published online February 26, 2015 (http://www.sciencepublishinggroup.com/j/mc)
doi: 10.11648/j.mc.s.2015030101.13
ISSN: 2329-1818 (Print); ISSN: 2329-180X (Online)

Synthesis and Characterization of Metal Complexes of Schiff's Base Ligands Derived from 4-Carboxy Hydrazide-5, 6-Diphenyl-3[2-H]Pyridazone

Faten Z. Mahmoud[1, *], Atef A. T. Ramadan[2], Mohamed M. Mahmoud[2], Fouz M. Omar[2]

[1]Chemistry department, University College for Girls, Ain Shams University, Cairo, Egypt
[2]Chemistry department, Faculty of Education, Ain Shams University, Cairo, Egypt

Email address:
faten_zm@yahoo.com (F. Z. Mahmoud)

To cite this article:
Faten Z. Mahmoud, Atef A. T. Ramadan, Mohamed M. Mahmoud, Fouz M. Omar. Synthesis and Characterization of Metal Complexes of Schiff's Base Ligands Derived from 4-Carboxy Hydrazide-5, 6-Diphenyl-3[2-H]Pyridazone. *Modern Chemistry*. Special Issue: Synthesis and Microbial Screening of Coordination and Organic Compounds. Vol. 3, No. 1-1, 2015, pp. 15-26. doi: 10.11648/j.mc.s.2015030101.13

Abstract: A new ligand, 4-[carboxy-α-(2-hydroxyphenyl) ethylidene hydrazide-5,6-diphenyl-3(2H) pyridazinone (CHDP), were synthesized and characterized by ^{1}H-NMR, IR spectra and elemental analysis. The dissociation equilibrium constant of CHEDP as well as the equilibrium constant for different M^{+n}-CHEDP complexes were reported at different temperatures in 75% (v/v) dioxane-water media and constant ionic strength. The stability constants of CHDP complexes with transition and non-transition ions were evaluated. The thermodynamic parameters were also calculated and discussed. A series of mono nuclear protic M(HL), $M(HL)_2$, ML(HL) and non-protic ML_2 complex species were formed in solutions. The structure of the solid complexes formed between CHEDP and cobalt (II), copper (II) and iron (III) are substantiated by elemental analysis, mass spectra, thermal studies (TG and DSC) and IR spectra.

Keywords: CHEDP Ligand, Potentiometric Titration, Spectrophotometric Studies of Fe (III)- CHEDP Complexes, Solid Complexes

1. Introduction

Pyridazines are compounds act as complexing agents, 2-hydrazino pyridazine and their metal complexes have many analytical application and also of a great interest in various biological systems [1,2].

The synthesis of pyridazine hydrazines may lead to prepare several interesting chelating agents [3:5]. The condensation reaction takes place between hydrazine group and carbonyl group to give ligand with chromophoric group (1). These classes of compound are structurally related to the corresponding azo-pyrazolone dyes (II) and different only on the position of azo- or hydrazo- group relative to the nitrogenous nucleus [6,7].

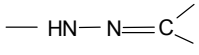

(I)

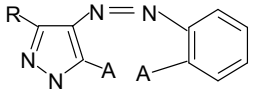

(II)

In the present communication, the metal complexes formed with 4-[carboxy-2-hydroxybenzylidene]-5,6-diphenyl-3-(2H)-pyridazinone (CHDP) and 4-[carboxy-α-(2-hydroxyphenyl) ethylidene hydrazine-5,6-diphenyl-3(2H) pyridazinone (CHEDP) are discussed.

2. Experimental

2.1. Materials

All chemicals were commercial product of analytical grade. Solvents were purified by conventional methods. The parent compound 4-carboxy hydrazide-5,6-diphenyl-3-(2H) pyridazinone was synthesized as previously described [8].

2.2. Preparation of Ligands

CHEDP and CHDP were obtained by mixing 100 ml of ethanolic solution of 0.01 mole of 4-carboxy hydrazide-5,6-diphenyl-3-(2H) pyridazinone and 0.012 moland e of o-hydroxy acetophenone and o-hydroxy salicylaldehyde, respectively. The reaction mixture was refluxed for three

hours. Then the formed solid was crystallized from ethanol to give CHEDP, m. p. 255, 167°C, respectively.

2.3. Synthesis of the Complexes

Table (1). *Analytical data and general behavior of CHDP complexes.*

Compound	Colour	Found (Calc.)				$\mu_{eff.}$ (B.M.)	Conductance (μS/cm)
		C	H	N	M		
CHDP		67.60 (67.29)	4.60 (4.67)	13.16 (13.08)			
CHEDP		67.50 (67.87)	4.80 (4.78)	12.55 (12.67)			
$[Cu(C_{24}H_{17}N_4O_3)(H_2O)_3(NO_3].H_2O$ *M. W. = 606.55 ** 601	Green	47.71 (47.49)	4.22 (4.12)	11.35 (11.54)	10.50 (10.48)	1.82	15
$[Co(C_{24}H_{17}N_4O_3)\ (H_2O)_3]NO_3.H_2O$ *M. W. 601.90 ** 602	Orange	48.20 (47.93)	4.00 (3.94)	11.54 (11.65)	9.92 (9.80)	4.48	67
$[Fe(C_{24}H_{16}N_4O_3)(H_2O)_3]2H_2O.NO_3$ *M. W. 615.85 ** 603	Black	46.98 (46.84)	4.19 (4.07)	11.33 (11.38)	9.00 (9.08)	5.67	75.2

*molecular weight
** molecular weight (mass spectra data)

Copper (II), Co(II) and Fe(III) chelating were prepared by adding ethanolic solution of CHDP ligand (≈ 0.01 moles) to aqueous solution of metal nitrate (0.01 moles). The mixture was refluxed for one hour. The solid obtained has filtered off, washed and dried, the elemental analysis of the complexes are given in Table 1. Also, the complexes were analyzed for their metal content by EDTA titrations using suitable indicator.

2.4. Measurements

Potentiometric studies were done with WTW digital pH-meter with a combined glass electrode. Solutions were adjusted to 0.10M ionic strength by addition of KNO_3 and maintained at constant temperature (±0.05°C) with constant temperature water circulated through a sealed of jacketed cell. The ligand solution in 75% (v/v) dioxane-water reached with standard carbonate-free KOH in 75% (v/v) dioxane-water and the pH had recorded after addition of each increment of base. Metal-chelate formation equilibriums were measured with 3:1 molar ratios of the ligand to metal ion (0.001 M). The correction of pH value in 75% (v/v) dioxane-water was taken as +0.28 [9].

Infrared spectra (KBr discs) were recorded on a Perkin-Elmer 437 spectrometer (4000-400 cm^{-1}). The electronic spectra were measured at 25°C with Jasco V-550 UV-visible spectrometer, with 1 cm matched quartz cells. ^{1}H-NMR spectra were recorded on Varian EM-390, 90 MHZ. NMR-spectrometer with TMS as an internal standard.

Conductance of $1x10^{-3}$ M solution of the solid complex in DMF was measured using WTW D-812 Weil heium conductivity meter model LBR, fitted with cell model LTA 100.

Magnetic moments were measured by the Gouy method at room temperature using Johnson Matthey A/80 Product, model no. M KI, magnetic susceptibility balance with Hg $[Co(CNS)_4]$ as celibrant. Diamagnetic correction was calculated from Pascal's constants. The effective magnetic moment M_{eff} was determined according to: $M_{eff} = 2.828(X_M^{corr}.T)^{1/2}$, where X_M being the corrected molar magnetic susceptibility in e. m. u, mol^{-1} and T in K.

Thermal analysis (TG-DSC) was carried out on Shim adzu-5O thermal analyzer at heating rate 10°C/min in nitrogen atmosphere using TA-SO WSI program. Mass spectra were recorded on a Hewlett-Packard mass spectrometer; model MS 5988, electron energy 70 eV.

3. Results

3.1. Ligand Protonation Constant

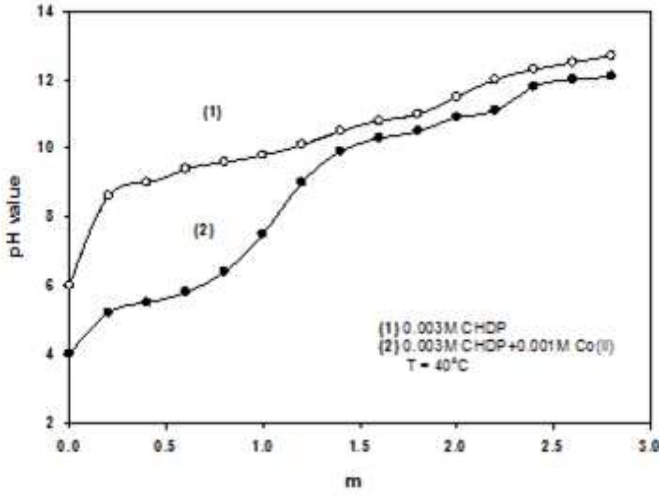

Fig. 1. *Potentiometric equilibrium curves for CHDP in absence and presence of Co(II)*

The protonation constants (pK_n^H, n = 1,2,3,…) of the ligand CHDP and CHEDP are determined by direct poteniometric measurements. A representative titration curves for CHDP in the absence and presence of some metal ion is plotted in Fig. 1. No conclusion about the protic nature

or the stepwise dissociation of OH and NH protons could be drowned from the titration curves of the free ligands. The protic nature of the ligands is substantiated from the metal-ligand titration curves, only two protons were liberated as indicated by the inflection point at m = 2 (m is the number of moles of base added per mole of metal). This indicates that under these conditions the ligand behaves as a diprotic species. For general protonation equilibrium:

$$H^+ + H_{n-1}L \Leftrightarrow H_nL \qquad \text{(n= 1 or 2)} \qquad (1)$$

The constants (K_n^H) were determined from hydrogen ion concentration of the ligand solution for each increment of the base added. The absence of any inflection point in the titration curves of the free ligand indicates that the protonation constants of –OH and –NH groups are close to each other (less than 2.8). The values of K_1^H (-OH) and K_2^H (-NH) are calculated from potentiometric data [10]. Since, the value of the ionic product of water in 75% (v/v) dioxane-water medium is 18.7 [11], both hydrogen and hydroxide ions concentration are negligible in the dissociation region.

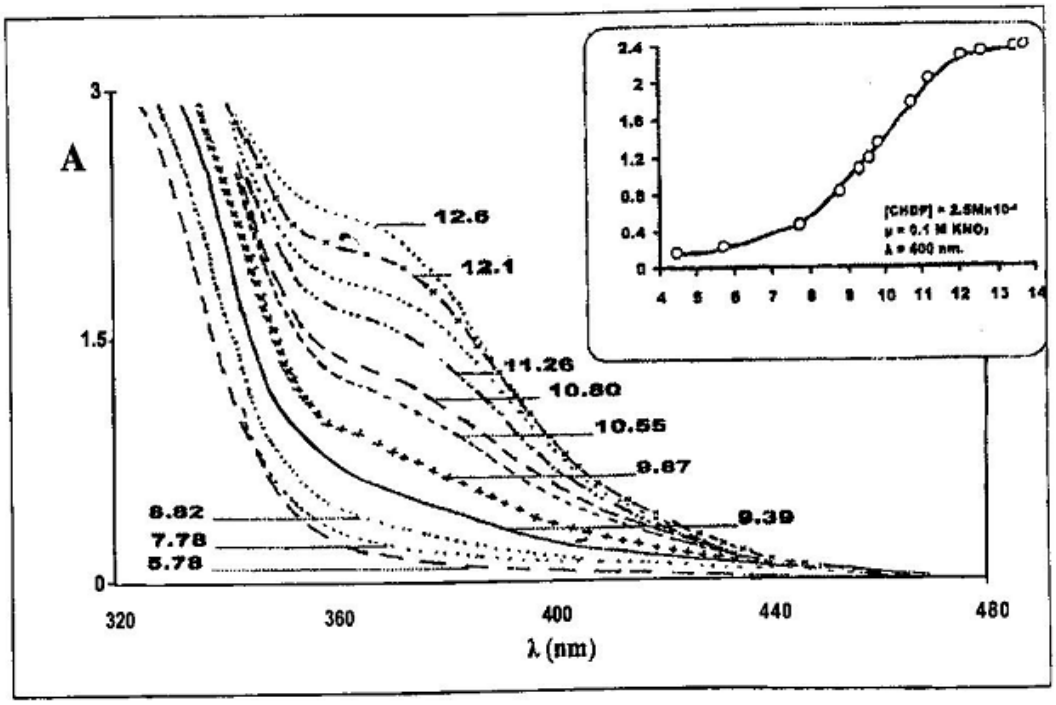

Fig. 2. *Electronic spectra of CHDP at different pH values*

In addition to pH-metric method, spectrophotometric method is further assessed for the calculation of protonation constants. The electronic absorption spectra of CHDP in 75% (v/v) dioxane-water display three absorption bands at 321, 275 and 220 nm and having molar absorptivities 2.00x10^4, 3.75x10^4 and 1.30x10^5 mol^{-1}.cm^{-1} respectively, like those reported for pyridazine ring at 245 and 295 nm [10]. The two bands at 275 and 321 nm in CHDP spectra are attributed to enhanced π→π* transition (K-band) over the whole conjugation system and an enhanced n→π* transition (R-band) respectively. At fixed lignd concentration, the absorbance was found to be pH-dependent Fig. 2. The results were analyzed for the calculation of the protonation constants of CHDP in 75% (v/v) dioxane-water using the following equation [10].

$$\frac{[H^+]}{K_1^H} x \frac{(\varepsilon - \varepsilon_C)}{(\varepsilon - \varepsilon_A)} + K_2^H = -[H^+] x \frac{(\varepsilon - \varepsilon_M)}{(\varepsilon - \varepsilon_A)} \qquad (2)$$

where, $\varepsilon_C, \varepsilon_A$ and ε_M are the molar absorptivities (extinction coefficient) for the analytical wavelength at given pH for di-protonated, mono-protonated and non-protonated species respectively.

The plot of $[H^+]\frac{(\varepsilon - \varepsilon_M)}{(\varepsilon - \varepsilon_A)}$ versus $[H^+]\frac{(\varepsilon - \varepsilon_C)}{(\varepsilon - \varepsilon_A)}$ gives straight line of slope equals to $(-1/K_1^H)$ and intercept equal (K_2^H). The values of K_1^H and K_2^H are refined using least square method. The obtained values are found to be 9.70 and 10.87 for K_1^H and K_2^H respectively compared to 9.71 and 10.82 obtained potentiometrically.

3.2. Ligand-Metal Ion Interactions

The protonation equilibrium curve for Co-CHDP at 40^{o}C is shown in Fig. 1. The shapes of these curves clearly indicate the formation of simple mononuclear chelate as well as various protonated species. The complex equilibrium in the first buffer region may be represented by:

$$M^{z+} + H_2L \Leftrightarrow M(HL)^{(z-1)+} + H^+ \qquad (3)$$

$$M(HL)^{(z-1)+} + H_2L \Leftrightarrow M(HL)_2^{(z-2)+} + H^+ \qquad (4)$$

Further addition of base results the subsequent dissociation

of two protons as indicated by the amount of base required per metal chelate. The reaction involved may be described by the equilibriums:

$$M(HL)_2^{(z-2)+} \Leftrightarrow ML(HL)^{(z-3)+} + H^+ \text{ and}$$
$$ML(HL)^{(z-3)+} \Leftrightarrow ML_2^{(z-4)+} + H^+$$

$$K^H_{M(HL)_2} = \frac{[M(HL)_2^{(z-2)+}]}{[ML(HL)^{(z-3)+}][H^+]} \quad (5)$$

$$K^H_{ML(HL)} = \frac{[ML(HL)^{(z-3)+}]}{[ML_2^{(z-4)+}][H^+]} \quad (6)$$

Computer assisted algebraic method use to solve the overlapping complex protonation constants involved in the second buffer regions. Calculation of the constants $K^M_{M(HL)}$ *and* $K^M_{M(HL)_2}$ was carried out using standard procedures based on the calculation of the average number of the ligand bound per metal ion (n^-_{HL}) and the free ligand concentration $[HL^-]$ using the first buffer region of the titration curve. Values of the constants are obtained from the intercept and slope of the linear relationship:

$$\frac{n^-_{HL}}{(1-n^-_{HL})[HL]} = \frac{(2-n^-_{HL})}{(1-n^-_{HL})} xK^M_{M(HL)_2} + K^M_{M(HL)} \quad (7)$$

The best straight line is obtained by the method of least squares. In a similar way, the second buffer region in the titration curves is used to calculate the constants $K^M_{ML(HL)}$ and K^M_{ML} as well as the constants $K^H_{ML(HL)}$ and $K^H_{ML_2}$. The values of stability constants as well as thermodynamic parameters were summarized in Tables 2, 3, 4, 5 and 6.

Table (2). *Protonation constants and thermodynamic parameters of CHDP and CHEDP ligands at different temperatures [75% (v/v) dioxane-water, μ = 0.1M KNO_3]*

Ligand	Symbol of proton constant	Protonation constant				ΔG	ΔH	ΔS
		10°C	20°C	30°C	40°C	Kcal/mole		Cal/mole.K
CHDP	pK^H_1	10.72	10.37	10.17	09.71	14.11	13.76	+1.2
	pK^H_2	12.18	11.82	11.63	10.82	16.11	19.12	-9.9
CHEDP	pK^H_1	11.09	10.76	10.11	09.95	14.03	16.51	-8.2
	pK^H_2	12.45	12.14	11.93	11.17	16.55	16.26	+1.0

Table (3). *Equilibrium constants and thermodynamic parameters for the interaction of CHEDP with nickel (II) ions [75% (v/v) dioxane-water, μ = 0.1M KNO_3]*

Symbol	Equilibrium quotient	Log (equil. Const.)				-ΔG	-ΔH	ΔS Cal/mole.K
		10°C	20°C	30°C	40°C	Kcal/mole		
$K^M_{M(HL)}$	$\frac{[M(HL)^{(z-1)+}]}{[M^{z+}][HL^-]}$	8.52	7.98	7.68	7.18	10.65	17.07	-21.2
$K^M_{M(HL)_2}$	$\frac{[M(HL)_2^{(z-2)+}]}{[M^{z+}][HL^-]^2}$	7.98	7.08	6.74	5.65	9.35	29.74	-67.3
$K^M_{ML(HL)}$	$\frac{[ML(HL)^{(z-3)+}]}{[M^{z+}][L^{2-}][HL^-]}$	7.30	6.17	5.33	3.97	7.39	46.05	-127.6
$K^M_{ML_2}$	$\frac{[ML_2^{(z-4)+}]}{[M^{z+}][L^{2-}]^2}$	6.26	5.19	4.50	3.28	6.24	39.78	-110.7
$K^H_{M(HL)_2}$	$\frac{[M(HL)_2^{(z-2)+}]}{[ML(HL)^{(z-3)+}][H^+]}$	8.04	8.93	9.61	10.18	13.33	-28.33	-137.5
$K^H_{ML(HL)}$	$\frac{[ML(HL)^{(z-3)+}]}{[ML_2^{(z-1)+}][H^+]}$	8.52	9.56	10.27	11.43	14.25	-38.65	175.6

ΔG ± (0.08-0.22), ΔH ± (0.01-0.49), ΔS ± (0.1-1.0)

Table (4). *Relation between 2nd I. P. and free energies of formation constants for some transition metal-CHEDP chelates.*

Cation M^{2+}	2nd I. P.	$-\Delta G^M_{M(HL)}$	$-\Delta G^M_{M(HL)_2}$	$-\Delta G^M_{ML(HL)}$	$-\Delta G^M_{ML_2}$	$-\Delta G^H_{M(HL)_2}$	$-\Delta G^H_{ML(HL)}$
Cu	20.25	13.710	12.930	07.01	06.010	13.61	15.190
Ni	18.18	10.650	09.350	07.39	06.240	13.33	14.250
Co	17.03	09.750	07.750	07.41	06.160	13.61	15.190
Zn	17.96	10.150	08.790	06.92	06.252	14.81	17.668
Mn	15.65	07.580	06.540	06.20	05.420	14.52	16.630
Cd	16.22	08.112	07.256	06.52	05.592	14.54	15.820

Table (5). *Relation between 2nd I. P. and enthalpy change of formation constants for some transition metal-CHEDP chelates.*

Cation M^{2+}	2nd I. P.	$-\Delta H^{M}_{M(HL)}$	$-\Delta H^{M}_{M(HL)_2}$	$-\Delta H^{M}_{ML(HL)}$	$-\Delta H^{M}_{ML_2}$	$-\Delta H^{H}_{M(HL)_2}$	$-\Delta H^{H}_{ML(HL)}$
Cu	20.25	18.570	43.930	42.200	38.760	-20.590	-20.530
Ni	18.18	17.070	29.740	46.050	39.780	-28.330	-38.650
Co	17.03	14.280	25.210	38.620	29.510	-29.490	-34.480
Zn	17.96	14.942	28.245	41.675	33.442	12.693	-25.999
Mn	15.65	10.268	19.551	31.153	25.711	13.633	-10.434
Cd	16.22	11.958	23.655	33.378	27.275	13.010	08.658

Table (6). *Entropy values for some transition metal-CHEDP complex systems*

Cation M^{2+}	$-\Delta S^{M}_{M(HL)}$	$-\Delta S^{M}_{M(HL)_2}$	$-\Delta S^{M}_{ML(HL)}$	$-\Delta S^{M}_{ML_2}$	$-\Delta S^{H}_{M(HL)_2}$	$-\Delta S^{H}_{ML(HL)}$
Cu	16.0	102.3	96.6	104.8	-24.0	-17.6
Ni	6.4	67.3	121.1	106.9	-49.5	-80.5
Co	4.5	57.6	101.8	72.9	-52.4	-63.7
Zn	4.8	64.2	104.0	87.5	90.0	-27.5
Mn	2.7	42.9	77.8	64.4	92.9	20.5
Cd	3.9	54.1	83.3	68.6	90.9	80.8

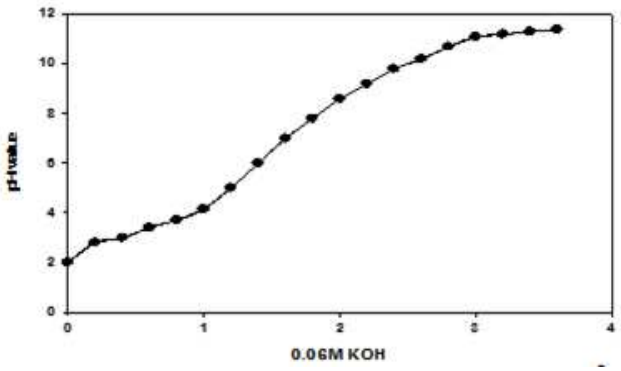

Fig. 3. *Potentiometric equilibrium curve of 1:3 molar ratio of Fe^{+3}ion to CHDP in 75% (v/v) dioxane-water solvent*

The poteniometric equilibrium curves of the Fe(III)-CHDP and Fe(III)-CHEDP systems show a curve similar to strong acid titration Fig. 3. The formation of iron chelate is so nearly complete even at low pH, that the stability constant can not be accurately calculated from poteniometric data. For this reason, the values of stability constants for Fe(III)-CHDP and Fe(III)-CHEDP have been determined by spectrophotometric method.

On mixing a solution containing Fe(III) ions with the solution of CHDP in 75% (v/v) dioxane-water, coloured complexes are formed. At constant metal ion concentration [Fe^{3+}] and varying ligand concentration, the absorbance increasing effectively at low concentrations of ligand but tends to attain a limiting value at higher concentrations Fig. 4. Multiple band spectra indicate the probable formation of complexes with varying stiochiometry. The intensities of peaks observed are function of both pH of the medium and the molar ratios of metal to ligand. As seen from Fig. 5, the absorbance increases rapidly with increase pH from 2 to 4, followed by a plateau in pH region 4.0 - 9.0. From the absorbance-pH diagram, it can be concluded that the optimum pH values are ≈3.0 for the formation of Fe(III)-CHDP complex systems. In addition, it could be concluded that more than one species are formed. At pH 2.0, the formation of protonated complexes $[Fe(HL)]^{2+}$ and $[Fe(HL)_2]^{1+}$ are formed through the replacement of phenolic proton. On increasing the pH from 2.0 to 4.0, the ionization of NH proton could take place and this leads to the formation of different species. These different absorbing species in the pH range from 2.0 to 9.0 is substantiated applying Coleman's graphical method [13]. Typical plots are given in Fig. 6 "a &b". The analysis revealed that only one absorbing species exists in the acidic region (pH below 4.0), which probably formed between Fe(III) and acidic ligand Fig. 6a. Above pH 4.0 two absorbing species (protonated and non-protonated) are found as indicated by the linear plots shown in Fig. 6b. Above pH 6.0, the absorbance is nearly constant indicating that both the protonated [ML(HL)] and non-protonated [ML_2] are absorbing to the same extent $(\varepsilon_{ML(HL)} \approx \varepsilon_{ML})$.

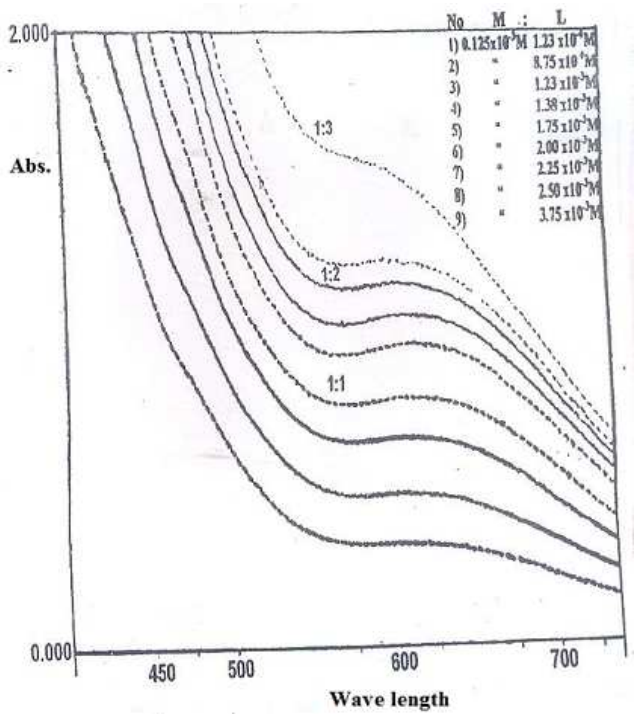

Fig. 4. *Electronic spectra of Fe^{3+}-CHDP complex in 75% (v/v) dioxane-water solvent*

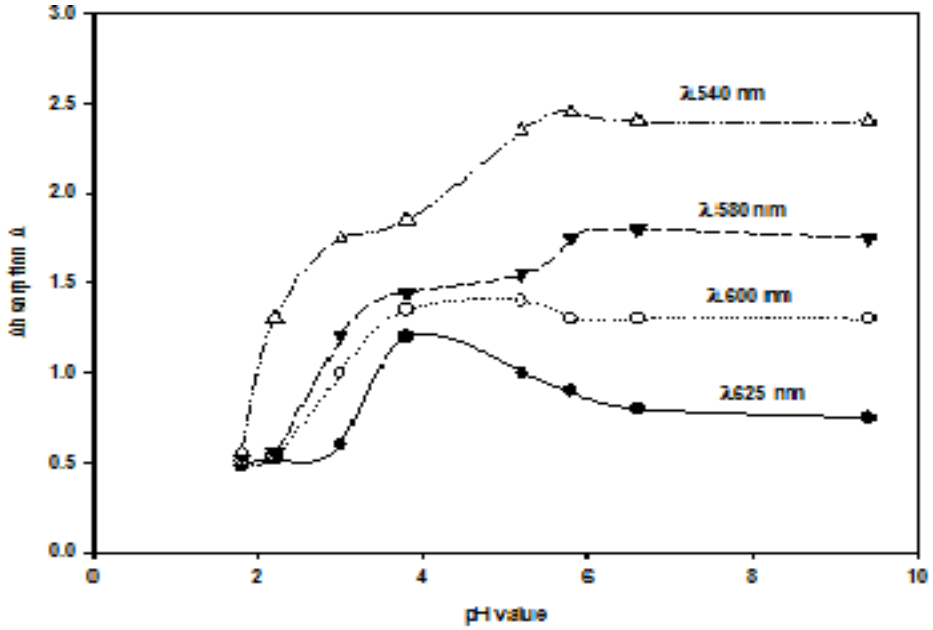

Fig. 5. *Absorbance vs. pH plots for Fe(III)-CHDP Chelates*

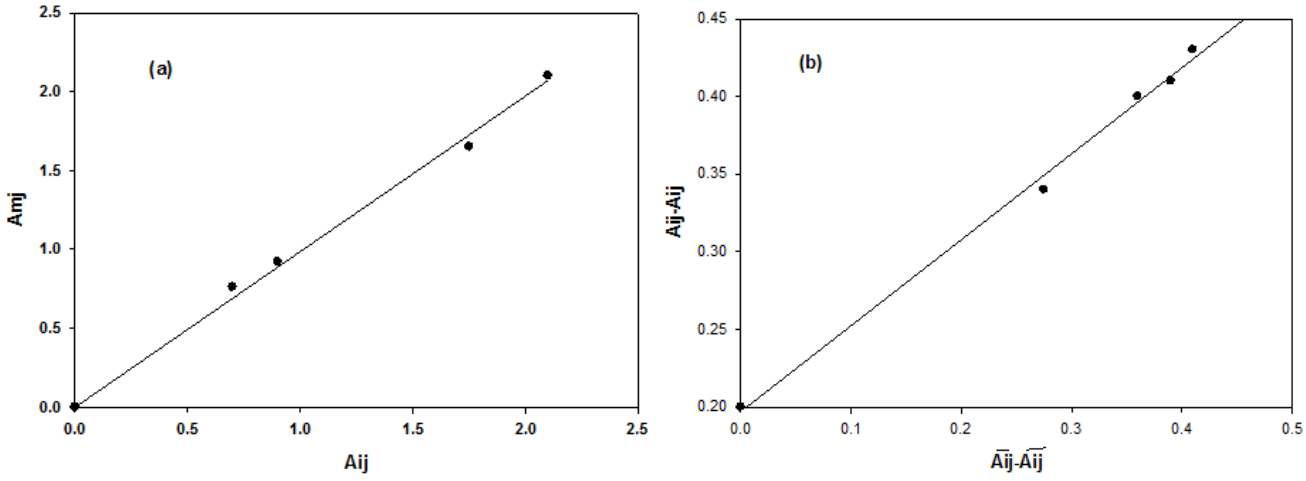

(a) pH: 0.4-3.77 (b) pH: 4.00-9.00

Fig. 6. *Colman et. Al. plots for different Fe(III)-CHDP chelates*

The composition of complexes formed in this study is determined using Job's and molar ratio methods [14]. All of these spectrophotometric methods indicate the formation of 1:1 and 1:2 (M:L) complexes. In molar ratio method, a sharp break in the line at 1:1 and 1:2 (M:L), indicating formation of 1:1 and 1:2 complex types. In Job's method the curve shows maximum absorbance at 0.5 mole fraction indicating the presence of 1:1 (M:L) complex type.

For studying the validity of Beer's law, a series of solutions containing constant excess concentration of ligand (CHDP or CHEDP) and variable concentration of Fe(III) ions all in 75% (v/v) dioxane-water are prepared. The absorbance of these solutions is measured at fixed wavelength (usually λ_{max}) the linear relation obtained between $C_{Fe^{3+}}$ and absorbances satisfy Beer's law for iron in certain concentration range. Values of ε are 1309.5 and 601.5 mol^{-1} cm^{-1} at 625 nm and optimum range for accurate measurement are $1x10^{-4} \approx 1.2x10^{-3}$ and $1x10^{-4} \approx 2.6x10^{-3}$ for CHDP and CHEDP complex systems respectively. These ranges had obtained from Ringbom plots and Sandell's sensitivity index [15], S% = $2.14x10^{-3}$ and $4.65x10^{-3}$ for Fe(III)-CHDP and Fe(III)-CHEDP complex system respectively. The reproducibility of the method is checked by testing three series of solutions and the relative standard deviation is found to be less than 2%.

Since iron chelates have intense colors and absorb in the region 500-600 nm, the formation constants of these species were calculated spectrophotometrically. In the region of overlapping spectrograms of the free metal ion and its complex, assuming that only 1:1 complexes are formed $(C_L / C_M < 0.3)$, the following relationship holds for Fe(III)-CHEDP complex system [16]:

$$[HL^{-1}]^{-1} = (1 - A/A_o)(K^M_{M(HL)} - \alpha) - K^M_{M(HL)} \quad (8)$$

where, A, Ao are the absorbance in the absence and presence of the ligand. $\alpha = K^M_{M(HL)} x(\varepsilon_C / \varepsilon_M)$ where, $\varepsilon_C and \varepsilon_M$ are the molar extinctions of the complex and metal ion respectively. Plots of $[HL^{-1}]$ vs. $(1 - A/A_o)$ gives a straight line its intercept is $-K^M_{M(HL)}$.

The free ligand concentration were calculated at any particular pH using the following equation:

$$C_{HL^-} = [HL^-](1 + K^H_1[H^+] \quad (9)$$

A sample set of these calculations are shown in Fig. 7. In the region of overlapping spectrograms of Fe(III)-CHEDP complex and assuming that 1:1 complex is formed another equation is used to calculate the stability constant [17]:

$$\log K^M_{M(HL)} = \log(A/\varepsilon) - \log[HL] - \log[M] \quad (10)$$

where, A and ε are the absorbance and molar extinction of the complex. The value of $\log K^M_{M(HL)}$ for Fe(III)-CHEDP complex obtained by this method is 11.31±0.16 which is higher than the corresponding value for Fe(III)-CHDP complex system ($\log K^M_{M(HL)}$ = 10.20±0.15). This difference is consistent with the structure of the two ligands. In CHEDP, the methyl group increases the basicity of the ligand, which in turns increases its stability constant.

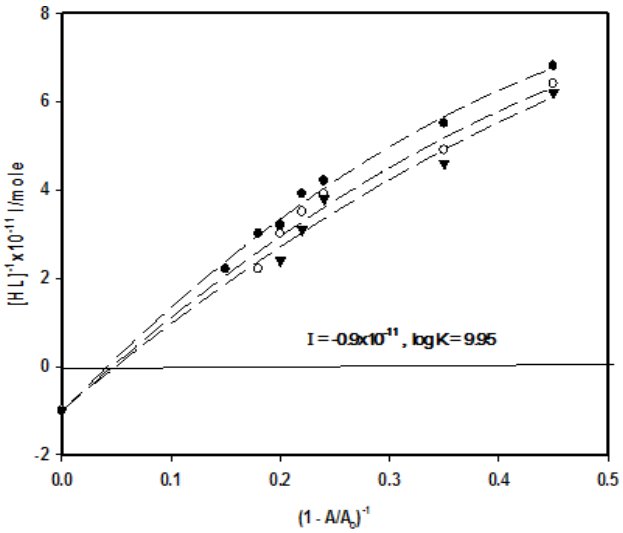

Fig. 7. *Nach's plot $[HL]^{-1}$ vs. $(1-A/A_o)$ for Fe(III)-CHDP, system in 75%(v/v) dioxane-water (A and A_o are absorbance in absence and present of ligand*

4. Discussion

4.1. The Ligand

Table 7. *Structural parameters of the ligands calculated using Hyper chem. 7-5 at PM3 level.*

	CHDP---H	**CHEDP---CH_3**
E_{total}	-107159.695	-110616.484
E_{HOMO}	-9.234	-9.1902
E_{LUMO}	-1.00386	-0.86597
Heat of formation	55.0445	41.3793
Dipole moment	3.357	5.402
Cl-N_2	1.326	1.326
N2-N3	1.343	1.342
N3-C4	1.431	1.433
C4=O33	1.223	1.222
C4-C5	1.467	1.467
C5-C19	1.491	1.490
C19=O20	1.209	1.219
C19-C21	1.488	1.434
C21-C23	1.396	1.389
C23-C24	1.293	1.303
C24-H34	1.099	---
C24-C25	1.469	1.479
C25-C26	1.408	1.406
C26-O31	1.366	1.368
O31-H35	0.9494	0.9492

Table 8. *Some important infra-red spectral bands of CHEDP and CHDP and its complexes (ν in cm^{-1}).*

CHEDP	CHDP	CHDP-Cu(II)	CHDP-Co(II)	CHDP-Fe(III)	Assignment
3500 b	3450 b	---	----	---	V_{OH} intermolecular H-bond
---	---	3520 b	3400 b	3425 b	V_{OH-H}
3200 b	3200 b	---	---	---	$V_{(N-H)}$
---	3058	3061	---	---	V_{C-H} aromatic
---	2927	2949	---	---	Saturated $V_{(N-H)}$
1680 s	1680 s	1710 m	1630 s	1654 s	$V_{C=O}$
1620 s	1620 s	1670 m	1610 s	1604 s	$V_{C=C}$
1510 s	1490 s	1500 m	1550 m	1538	$V_{C=N}$
1490 s	1440 m	1440 vs	1390 s	1439 w	$V_{N=N}$
1375 s	1370 s	1330 w	1350 m	1384 vs	$\nu_{C=N_2}$ *
1300 s	1310 m	1250 w	1280 m	1304 m	V_{C-C}
1250 s	1275 s	1200 w	1200 s	1204 m	V_{C-O}
1150 s	1190 mb	1180 w	1150 m	1150 w	$V_{C=N}$
1075 w	1130 mb	1075 w	1070 w	---	---
1020 m	1030 s	1010 w	1030	1028 w	---
980 m	960 vs	950 w	920 w	960	V_{N-N}
940 m	920 m	---	---	---	---
810 m	880 m	800 s	---	810 m	---
750 vs	750 s	750 s	750 s	755 vs	Substituted benzene ν_{C-H}
700 vs	690 s	690 s	---	670 vs	
640 m	---	---	---	---	---
600 m	---	650 w	650 w	604 m	Φ_{C-C} aromatic
---	---	580 w	600 w	551	V_{M-O} ; V_{M-N}
---	---	540 w	470 w	446	

s = strong ; m = medium ; w = weak ; b = broad ; v = very
frequency in cm-1
*the atoms are numbered in the structures

The analytical and spectral data prove that each ligand is a mixture of two tautomeric isomers is shown in the following diagram [12]:

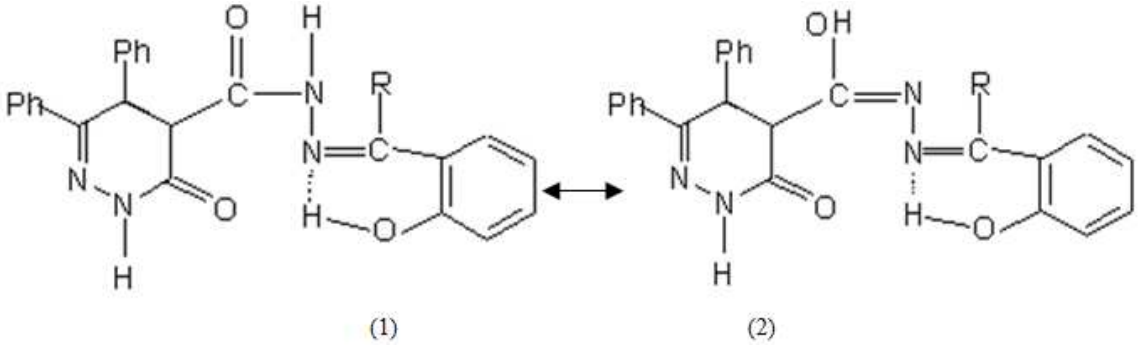

[R = -H→ CHDP], [R = CH_3→ CHEDP].

Thus the IR-spectrum of the ligands CHDP and CHEDP could be associated with both tautomeric isomers 1 and 2. The υ_{N-H}, $\upsilon_{C=N}$ and $\upsilon_{C=O}$ of tautomeric isomer 1 are detected at 3200, 1680 and 1620 cm^{-1} respectively (Table 8). The phenolic –OH is observed at 3450 and 3500 cm^{-1} as broad bands for CHDP and CHEDP respectively. The broadness of such band could be related to hydrogen bonding with –C=N group. Evidence for tautomeric structure 2 is derived from IR bands related to υ_{N-N} and υ_{C-O} which appeared at 980-960 and 1275-1280 cm^{-1} respectively.

The ^{1}H-NMR spectrum (DMSO-d6) of CHEDP shows at δ 2.2 (s, 3H, CH_3); 6.5-7.4 (m, 15H, Ar-H phenolic OH). 10.7 (s, 1H, exocycllic CONH) and 12.9 ppm (s, 1H, cyclic CONH). The structure of CHEDP compound was further confirmed by the mass spectrum which exhibited peaks at m/e 424 (78.34%) $[M^+C_{25}H_{20}N_4O_3]$; 409 (34.28%) $[C_{24}H_{17}N_4O_3]$; 378 (13.24%) $[C_{25}H_{18}N_2O_2]$; 290 (40.72%) $[C_{18}H_{14}N_2O_2]$; 275 (100%) $[C_{17}H_{11}N_2O_2]$; 247 (83.17%) $[C_{16}H_{11}N_2O_2]$; 219 (25%) $[C_{16}H_{11}O]$ and 203 (13.12%) $[C_{16}H_{11}]$. The base peak at m/e 275 (100%) is formed due to loss of ($C_{17}H_{12}N_2O_2$) from the parent ion peak of CHEDP, and the base peak at m/e 122 (100%) is formed due to loss of (C_7H_8NO) from the parent peak for CHDP.

Furthermore, the proposed structure of the ligands were optimized and structure parameters were evaluated by means of semi-empirical molecular obtained calculations of MP_3 level provided by hyper Chem. release 7.5. The calculated structural parameters data are summarized in Table 7. The heat of formation (ΔH_f), dipole moment, HOMO and LUMO entropies and ΔE_{gap}= (ΔE_{HOMO} - ΔE_{LOMO}) as well as bond

length. Analysis of the data indicates that the calculated heat of formation (ΔH_f) as well as ΔE_{gap} values of the present ligand, suggest that the more favorable toutomeric forms are shown in the following diagram

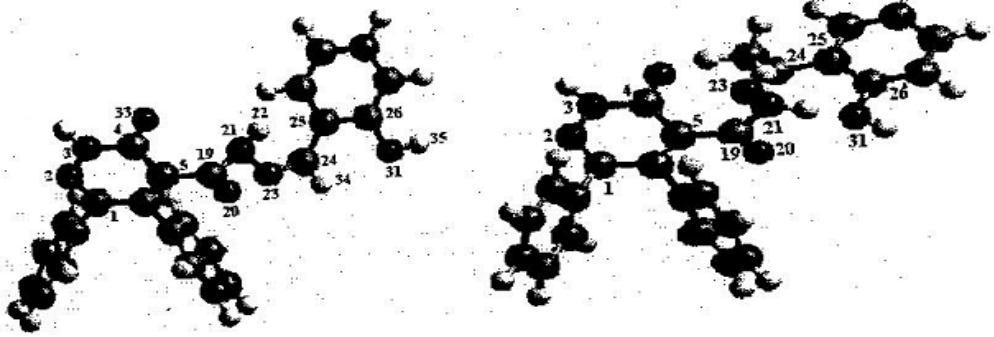

CHDP….H *CHEDP……CH_3*

4.2. Solid Complexes

4.2.1. Conductivity and Magnetic Properties

The metal complexes, which were isolated in the present study, are presented in Table 1 together with some of their properties. The deprotonation of hydrazo and phenolic protons occurs in 1:1 Fe(III)-CHDP while in cases of Cu(II)-CHDP and Co(II)-CHDP complexes only the phenolic group is deprotonated. The molar conductance values of 10^{-3}M complex solution in DMF are 15, 67.00 and 75.20 MS/cm for copper, cobalt and iron complexes respectively. This indicates that 1:1 electrolyte for cobalt and iron complexes, while nonionic nature for copper complex.

The magnetic moments (μ_{eff}) of iron (III) and cobalt (II) complexes are 5.67 and 4.41, which are normal and suggest octahedral geometry for them. The magnetic moment of copper (II) complexes reported here is in the range ≈ 1.8 B.M. accepted for Cu(II) complexes [18] (one unpaired electron).

4.2.2. IR Spectra of the Complexes

The infrared spectra of these solids show a systematic shift of $\upsilon_{C=C}$, $\upsilon_{C=N}$ and $\upsilon_{C=O}$ bands to lower frequency with the simultaneous disappearance of υ_{N-H} and υ_{O-H} bands. The υ_{O-H} band in the free ligand is not observed but is replaced by a broader band at 3400-3520 cm^{-1} in the spectrum of the complex due to υ_{O-H} of the coordinated water molecules. The participation of phenolic oxygen and azo-methane or N-H nitrogen are substantiated from the appearance of new bands at 551-580 and 340-470 cm^{-1} on the spectra of the solid complexes assigned to υ_{M-O} and υ_{M-N} respectively.

4.2.3. Thermal Analysis (TG-DSC)

The results of TG-DSC studies of CHDP ligand and its complexes Cu(II)-, Co(II)- and Fe(III)-CHDP are summarized in Table (9) at ambient temperature up to 800°C, the rate is 20°C per minute. The composition of intermediates proposed were the best fit of the observed weight loss. The TG curve of the free ligand as shows a very rapid and big mass loss (second step) in the range 198.86-437.62°C corresponding to the liberation of organic moiety $C_{17}H_{11}N_2O_2$ [found 63.74; calc. 64.25]. The exothermic peak at 400°C originates from the combustion of carbon from the organic part. The first decomposition stage starts at 44.41°C and continues until 198.86°C, corresponding to the degradation of $2H_2O$ molecules (one crystalline H_2O and the other from the ligand) constituting about 8.17 of the total weight loss (8.41 calc.)The third step show the decomposition of the remaining part of the molecule $C_7H_5N_2$ at 438.99-798.80°C temperature range (found: 27.65; calc. 27.34). DSC analysis was performed in order to obtain quantitative results for thermal effects accompanying various processes occurring during heating.

Table 9. *DTA and DSC data for CHDP complexes*

Compound	stage	Temperature range °C	Weight %		DSC peak		ΔH J/g	Product
			Found	Calc.	Endo	Exo		
$[Cu(C_{24}H_{17}N_4O_3)(H_2O)_3(NO_3)]H_2O$ 606.55	1	42.6-183.1	3.28	2.97		-120	-72.55	H_2O
	2	184.8-377.6	16.25	16.49	323		55.11	NO_2 ; $3H_2O$
	3	377.6-413.7	22.04	22.09	354		89.12	$C_7H_6ON_2$
	4	413.7-498.9	22.56	21.76	417			$C_{11}H_2O$
	5	498.9-565.2	22.38	23.25		-600		$C_6H_9N_2O_2$
		Above 565.2	13.43	13.11				CuO
$[Co(C_{24}H_{17}N_4O_3)(H_2O)_3]NO_3.H_2O$ 601.9	1	55.9-102.0	3.15	2.99	95.6		-62.2	H_2O
	2	102.0-143.5	3.20	2.99	147		-4.26	H_2O
	3	143.5-272.9	5.74	5.98	401		-87.37	$2H_2O$
	4	272.9-443.0	19.10	19.77	415		-98.23	C_7H_5NO
	5	443.0-604.5	36.35	36.22	466		-101.42	$C_{13}H_2N_2O_2$
	6	604.5-671.0	4.40	4.65	600		-73.16	CO
		Above 671	28.06	29.72				CoO

Compound	stage	Temperature range °C	Weight %		DSC peak		ΔH J/g	Product
			Found	Calc.	Endo	Exo		
[Fe ($C_{24}H_{16}N_4O_3$)(H_2O)$_3$]NO_3.2H_2O 615.85	1	34.3-152.0	10.29	10.39		-83.2	-54.47	NO_2 ; H_2O
	2	152.0-257.6	11.38	11.69	180.2		-15.11	4 H_2O
	3	257.6-401.0	19.80	19.97	333.4		-57.11	$C_6H_5NO_2$
	4	401.0-743.0	41.68	41.73	420.2			$C_{17}H_{11}N_3$
		Above 743.0	16.85	16.21				FeO ; CO

The measurements were carried out at nearly the same rate as used for TG investigation. The composition of TG and DSC analysis is a very useful tool in the investigation and characterization of thermal behavior of organic compound**.** The values of thermodynamic quantities with particular TG and DSC curves for [Fe($C_{24}H_{16}N_4O_3$)(H_2O)$_3$]NO_3.2H_2O, (Table 9). The transition enthalpy values give information about the dimensions of thermal effects, being a sum of all processes that taking place in the particular temperature range. The thermal parameters of conversion of 1 and 2 steps are not similar (H_1= -54.36 J/g and H_2 = -15.11 J/g) because they are connected with loss of H_2O and NO_2 for the first step while the second step four of coordination water molecules are lost. The transition enthalpy of steps (3) is high (H_3 = -57.11 J/g), which is due to release of $C_6H_5NO_2$ moiety.

In the thermo gram of the complex [Fe($C_{24}H_{16}N_4O_3$)(H_2O)$_3$]NO_3.2H_2O, there are four steps of weight losses from room temperature to 743.0°C. The complex lost 10.29 of its weight at 34.34-151.99°C due to the liberation of NO_2 and H_2O molecules (calc. 10.39). In the second step 4 molecules of coordinated water are lost (found 11.38 and calc. 11.69). The third step occurred at 259.6-401.0°C range is due to the loss of $C_6H_5NO_2$ moiety from the organic part of ligand molecule (found 19.80, calc. 19.97). The remaining weight loss 41.68 is for organic matter $C_{17}H_{11}N_3$ obtained at 401.01-742.99°C range (calc. 41.73). The remaining weight loss above 742.99°C is corresponding to the oxide molecules FeO and CO (found 16.85, calc. 16.21).

The TG curve of copper complex shows about five steps, the first one gives a weight loss about 3.28% (calc. 2.97) due to one mole of crystalline water and is characterized by an exothermic peak in the DSC curve at 120°C. The second step is due to loss of NO_2 and 3H_2O (found 16.25, calc. 16.49) and show an endothermic peak in DSC curve at 323°C. The other remaining steps were due to loss of $C_7H_6ON_2$, $C_{11}H_2O$ and $C_6H_9N_2O_2$ organic moieties. These steps are characterized by two endothermic and one exothermic peak in DSC curve. CuO is appeared as a final product above 565°C, (found 13.43, calc. 13.11).

In case of cobalt complex, the decomposition process was completed and cobalt oxide (CoO) is formed above 600°C. The first three steps are due to the loss of crystalline and coordinated water molecules.

4.2.4. Mass Spectra

The molecular formulas of the above complexes were substantiated through mass spectra. The iron(III) complex [Fe($C_{24}H_{16}N_4O_3$)(H_2O)$_3$]NO_3.2H_2O (F.w., 615.85) show the highest mass peak at 603, which agrees with the formula weight of the complex [Fe($C_{24}H_{16}N_4O_3$)(H_2O)$_3$]NO_3.1¼H_2O (F.w., 603). The fragmentation patterns of the iron complex shows a fragment due to hydrated ligand molecule ($C_{24}H_{17}N_4O_3$).¾H_2O at 423.

For cobalt complex [Co($C_{24}H_{17}N_4O_3$)(H_2O)$_3$]NO_3.H_2O of F.w. 601.9 the highest mass peak is at 602, which agrees with the formula weight of cobalt complex. The fragmentation patterns of the complex show fragment at 439 due the ligand molecule with 1¾ water molecules ($C_{24}H_{17}N_4O_3$)1¾.H_2O.

The mass spectrum of the copper complex [Cu($C_{24}H_{17}N_4O_3$)(H_2O)$_3$(NO_3]H_2O shows a peak at 603 which in agreement with molecular formula of the complex (606.55). From the above discussion, the structure of the three investigated complexes is shown in the following scheme:

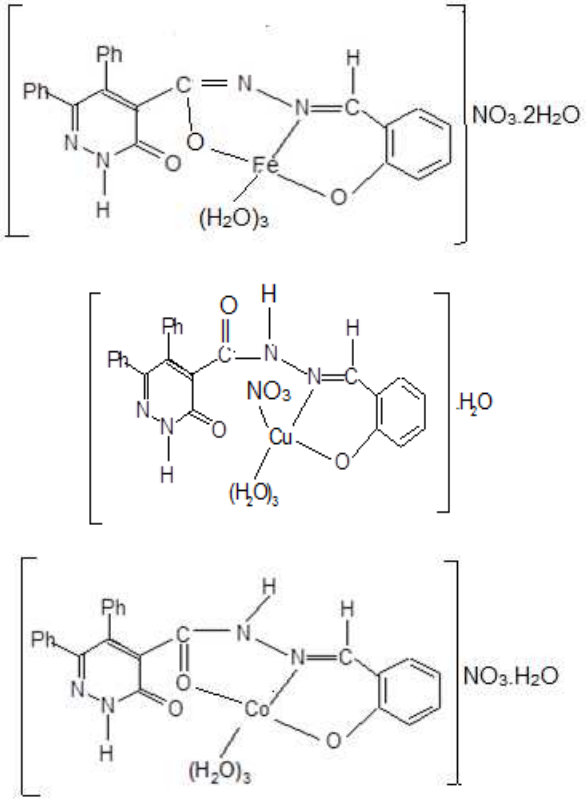

4.3. Complexes in Solution State

The values of acid dissociation constants K_1^H and K_2^H (phenolic –OH) and (hydrazo –NH) of CHEDP and CHDP ligands are not similar Table (2). This would indicate that the total inductive and hyper-conjugation effects of methyl group in CHEDP on the reagent basicity ($\sum K_1^H + K_2^H$) are mainly dependent on the presence of such methyl group. The

absence of this group in CHDP ligand could be account for the lower basicity of the ligand compared to CHEDP under similar conditions.

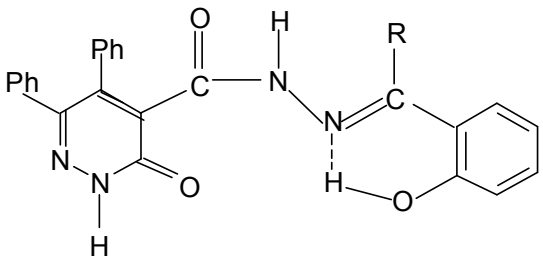

R = H in CHDP; R = CH_3 in CHEDP

All thermodynamic parameters of the dissociation process of the ligands are given in Table (2, 3). These values reveal that:

- The stepwise pK^H values decreasing with increasing temperature, demonstrating that its acidity increasing with increasing temperature.
- ΔH is positive indicating that dissociation is accompanied by absorption of heat and the process is endothermic.
- ΔG is positive indicating that the dissociation process is not spontaneous.
- ΔS is negative due to increased order as a result of salvation process.

The values of ΔG of protic and non-protic complexes formed between CHEDP and divalent metal ions are listed in Table (4). The relationship between ΔG for M(HL), $M(HL)_2$, ML(HL) and ML_2 complexes and second ionization potential of different metals is plotted in Fig. 8. The linear relation indicates that the two primary factors affecting the stability of the complexes formed between these ions and CHEDP are ionic radii and atomic number.

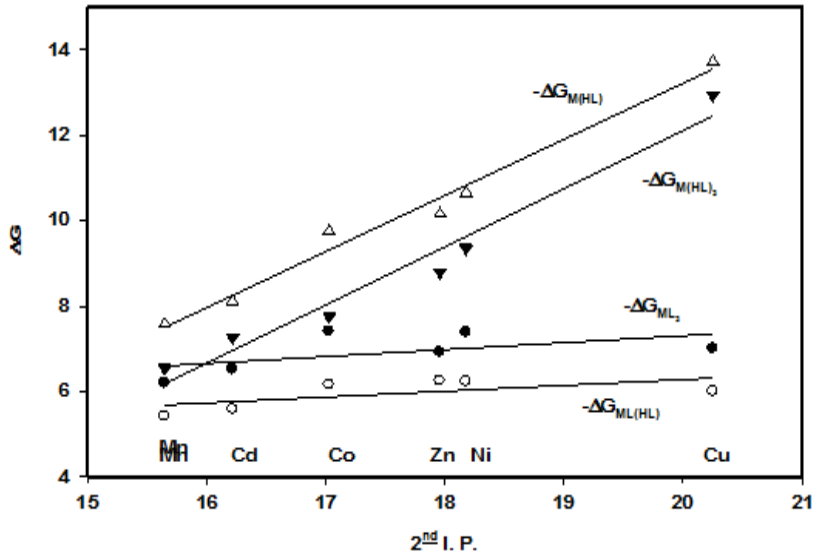

Fig 8. *Graphic relation between second ionization potential and free energy for some M^{+2}-CHEDP chelates*

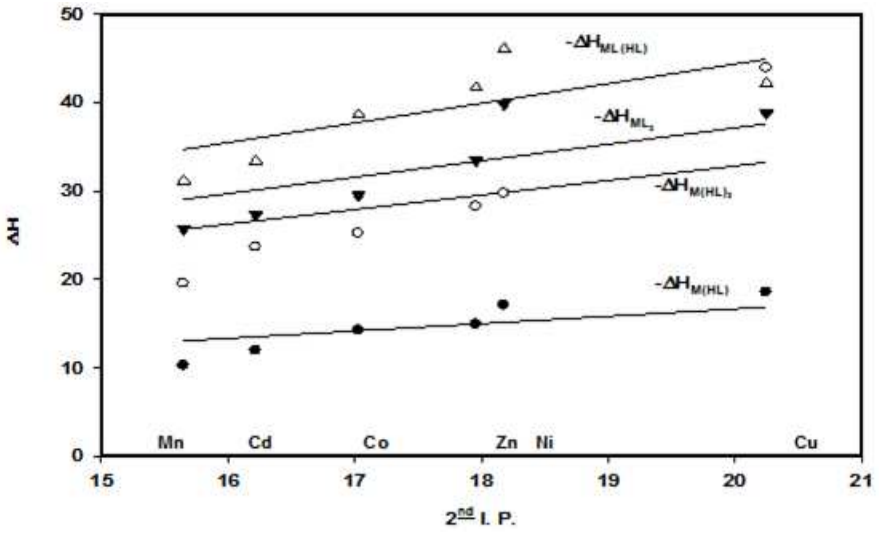

Fig. 9. *Graphic relation between second ionization potential and enthalpy change for some M^{+2}-CHEDP chelates*

The wide spread success of the relation between ΔH for the protic and non-protic complex species and second

ionization potentials of the metal ions shown in Fig. 9, indicates that the entropy of a series of chelation reaction with a given reagent will either be roughly constant or will vary regularly. This relationship is used because ΔH express bond strength, also the second ionization potential may be taken as a rough estimation of the average electron attracting power of a divalent metal ion. It will also be a measure of the attracting power of a divalent metal ion for a source of electrons such as that formed in the chelate ligand groups. Hence, it is more nearly related to bond energy and ΔH of chelation than ΔG as measured by log of chelate formation constants. It should also be noted that since in many cases ΔH are accompanied by opposing charge in ΔS. ΔH should be a more sensitive index of bond strength than ΔG. Fig. 9, shows a plot of second ionization potential of the gaseous metal atom against ΔH of chelation. As can be seen the relationship is satisfactory.

CHEDP forms MHL (protic) chelates as evidenced both by the titration curves and isolation of solid complexes. Probable arrangement of the order groups is shown in structure (III) with the M replacing H_1. As more base added, the pH becomes sufficiently high to assist in the dissociation of the second protons ($-H_2$). The basicity of this proton is not as strong as in the free ligands and influenced by the presence of metal ion in the following order: Ni < Co ≈ Cu < Zn < Mn < Cd, which is in a revised order of stabilities of the normal chelates.

References

[1] G. De Munno, G. Denti and P. Dapporte, Inorg. Chim. Acta, 74, (1983) 199-203.

[2] B. A. El-Shetary, M. S. Abdel-Moez and S. S. Sleem, Thermo Chemica Acta, 113, (1987) 21-29.

[3] A. A. T. Ramadan, M. H. Seada and E. N. Rizkalla, Talanta, 30, (1983) 245- 250.

[4] E. N. Rizkalla, A. A. T. Ramadan and M. H. Seada, Polyhedron, 2, (1983) 1155-1164.

[5] A. A. T. Ramadan, M. H. Seada and E. N. Rizkalla, Monatshefte fur Chemie, 116, (1985) 461- 477.

[6] F. A. Snavely, W. C. Fernelius and B. P. Block, J. Am. Chem. Soc., 79, (1957) 1028- 1030.

[7] Snavely, F. A., Krecker, B. D. and Clark, C. G.; J. Am. Chem. Soc. 81, (1959) 2337- 2338.

[8] M. H. Seada, M. M. Fawezy, H. Jahine, M. Abdel-Magid and R. R. Saad, J. Chin. Chem. Soc. 36 (1989) 241- 245.

[9] H. M. Irving and U. S. Mohanant, J. Inorg. Nucl. Chem. 30, (1968) 1215- 1220.

[10] A. Albert and E. P. Serjeant, "Ionization Constants of Acids and Bases" Chopman and Hall, Edinburgh, 1971.

[11] D. F. Goldberg, J. Chem. Educ. 40, (963) 341- 347.

[12] R. M. Sitverstein, G. O. Bassler and T. C. Morrill, "Spectrophotometric Identification of Organic Compounds" 4th Ed., Willey, New York, 1981.

[13] J. S. Colman, L. P. Varga and S. H. Martin, Inorg. Chem. 9, (1970) 1015- 1020.

[14] F. J. Rossotti and H. Rossotti, "Determination of Stability Constants", Mc Graw, Hill, New York, 1961.

[15] A. Bubko and A. Pilipenko, "Photometric Analysis" MIR Pub., Moscow, 227, (1971).

[16] C. P. Nach, Phys. Chem. Soc., 64, (1960) 950- 958.

[17] H. E. Bent and G. L. French, J. Am. Chem. Soc., 63, (1941) 568- 576.

[18] F. A. Cotton, and G. Wilkenson, "Advanced Inorganic Chemistry" 3th ed. Interscience, New York, 1972.